Cell Reports, Volume *43*

Supplemental information

Histone H3.1 is a chromatin-embedded redox sensor triggered by tumor cells developing adaptive phenotypic plasticity and multidrug resistance

Flavio R. Palma, Diego R. Coelho, Kirthi Pulakanti, Marcelo J. Sakiyama, Yunping Huang, Fernando T. Ogata, Jeanne M. Danes, Alison Meyer, Cristina M. Furdui, Douglas R. Spitz, Ana P. Gomes, Benjamin N. Gantner, Sridhar Rao, Vadim Backman, and Marcelo G. Bonini

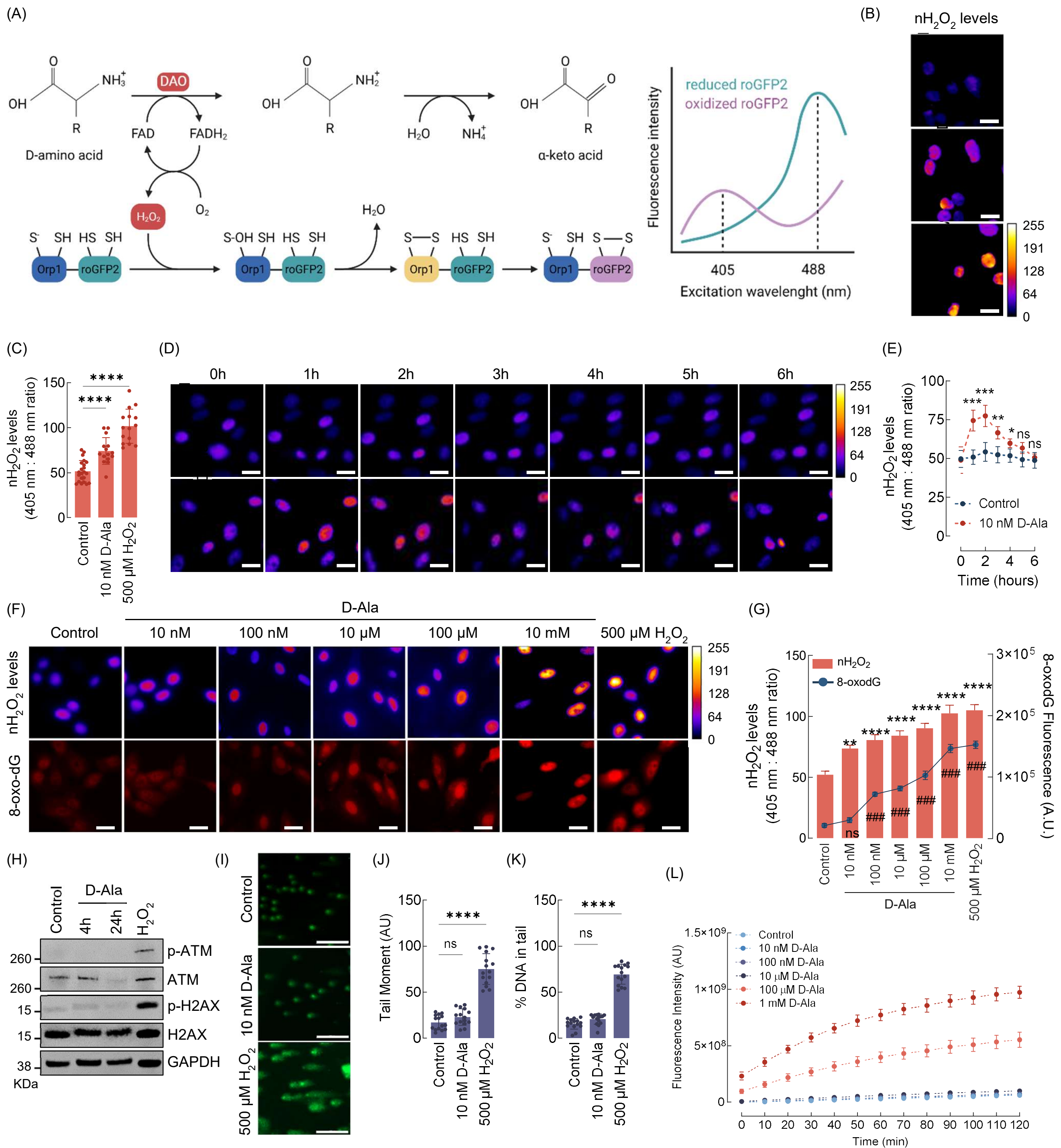

Figure S1. Model for generation and quantification of nuclear H_2O_2. *Related to Figure 1.*

(A) Schematic representation of our two-part system where nuclear H_2O_2 production by nuclear-targeted D-amino acid oxidase (NLS-DAO) is coupled to its quantification by the NLS-Orp1roGFP2 biosensor. Organelle-specific ROS production was achieved using D-amino acid oxidase (DAO), an enzyme that generates H_2O_2 as a byproduct of D-amino acid oxidation. To detect nuclear DAO-derived H_2O_2, the redox sensor Orp1-roGFP2 was used. Orp1 is oxidized

by H_2O_2 and subsequently oxidizes roGFP2. Oxidized (λ_{ex} = 405 nm) and reduced (λ_{ex} = 488 nm) roGFP2 signals are detected using fluorescence/confocal microscopy.

(B) D-Ala increases levels of nuclear ROS in cells expressing NLS-DAO. Images from MCF10A$^{ER/vSrc}$ cells were acquired 4h after treatment with 10 nM D-Ala or 30 min after treatment with 500 μm H_2O_2 (positive control). Levels of H_2O_2 in the nucleus were determined using confocal microscopy. Oxidized (λ_{ex} = 405 nm) and reduced (λ_{ex} = 488 nm) roGFP2 signals were acquired and the ratio oxidized/reduced was calculated using ImageJ (shown as a heatmap). White bars represent 20 μm.

(C) Quantification of oxidized:reduced ratio of nuclear Orp1-roGFP2 in (B). Statistical significance was determined by One-way ANOVA multiple comparison test with *post hoc* Tukey test. Bars represent mean ± SEM. ****$p<0.0001$.

(D) Time course of nuclear H_2O_2 levels in MCF10A$^{ER/vSrc}$ cells treated with 10 nM D-Ala. The levels of H_2O_2 in the nucleus were determined using confocal microscopy. Oxidized (λ_{ex} = 405 nm) and reduced (λ_{ex} = 488 nm) roGFP2 signals were acquired and the ratio oxidized/reduced was calculated using ImageJ (shown as a heatmap). White bars represent 20 μm.

(E) Quantification of oxidized:reduced ratio of nuclear Orp1-roGFP2 in (D). Statistical significance was determined by One-way ANOVA multiple comparison test with *post hoc* Tukey test. Bars represent mean ± SEM. *$p<0.05$, **$p<0.01$, ***$p<0.001$, ns - not significant.

(F) Nuclear H_2O_2 production assessed along with DNA damage. Different levels of D-Ala were tested to find a concentration that was sufficient to produce changes in NLS-Orp1roGFP2 but not to cause significant direct oxidative DNA damage as detected by 8-oxo-dG immunofluorescence. The levels of H_2O_2 and 8-oxo-dG in the nucleus of MCF10A$^{ER/vSrc}$ cells were determined using fluorescence microscopy 4h after D-Ala treatment and 30 min after treatment with 500 μm H_2O_2 (positive control). White bars represent 20 μm.

(G) Quantification of oxidized:reduced ratio of nuclear Orp1-roGFP2 (nH_2O_2 levels)and 8-oxo-dG in (F). Statistical significance was determined by One-way ANOVA multiple comparison test with *post hoc* Tukey test (with nH_2O_2 and 8-oxo-dG levels calculated separately). Bars represent mean ± SEM. **$p<0.01$, ****$p<0.0001$ (for nH_2O_2 levels) and $^{\#\#\#}p<0.001$, ns - not significant (for 8-oxo-dG levels).

(H) Western blot analysis of DNA damage markers. p-ATM and p-H2AX levels in MCF10A$^{ER/vSrc}$ cells were assessed by Western blot 4h or 24h after treatment with 10 nM D-Ala and 30 min after treatment with 500 μm H_2O_2 (positive control).

(I) Comet assay analysis of DNA strand breaks in MCF10A$^{ER/vSrc}$ cells 4h after treatment with 10 nM D-Ala and 30 min after treatment with 500 μm H_2O_2 (positive control). White bars represent 100 μm.

(J) Quantification of DNA damage by tail moment of comet assay [from (I)]. Statistical significance was determined by One-way ANOVA multiple comparison test with *post hoc* Tukey test. Bars represent mean ± SEM. ****$p<0.0001$, ns - not significant.

(K) % DNA in comet tails [from (I)]. Statistical significance was determined by One-way ANOVA multiple comparison test with *post hoc* Tukey test. Bars represent mean ± SEM. ****$p<0.0001$, ns - not significant.

(L) Extracellular H_2O_2 detection. MCF10A$^{ER/vSrc}$ cells were treated with different concentrations of D-Ala and the levels of H_2O_2 released to extracellular milieu was measured using Amplex red.

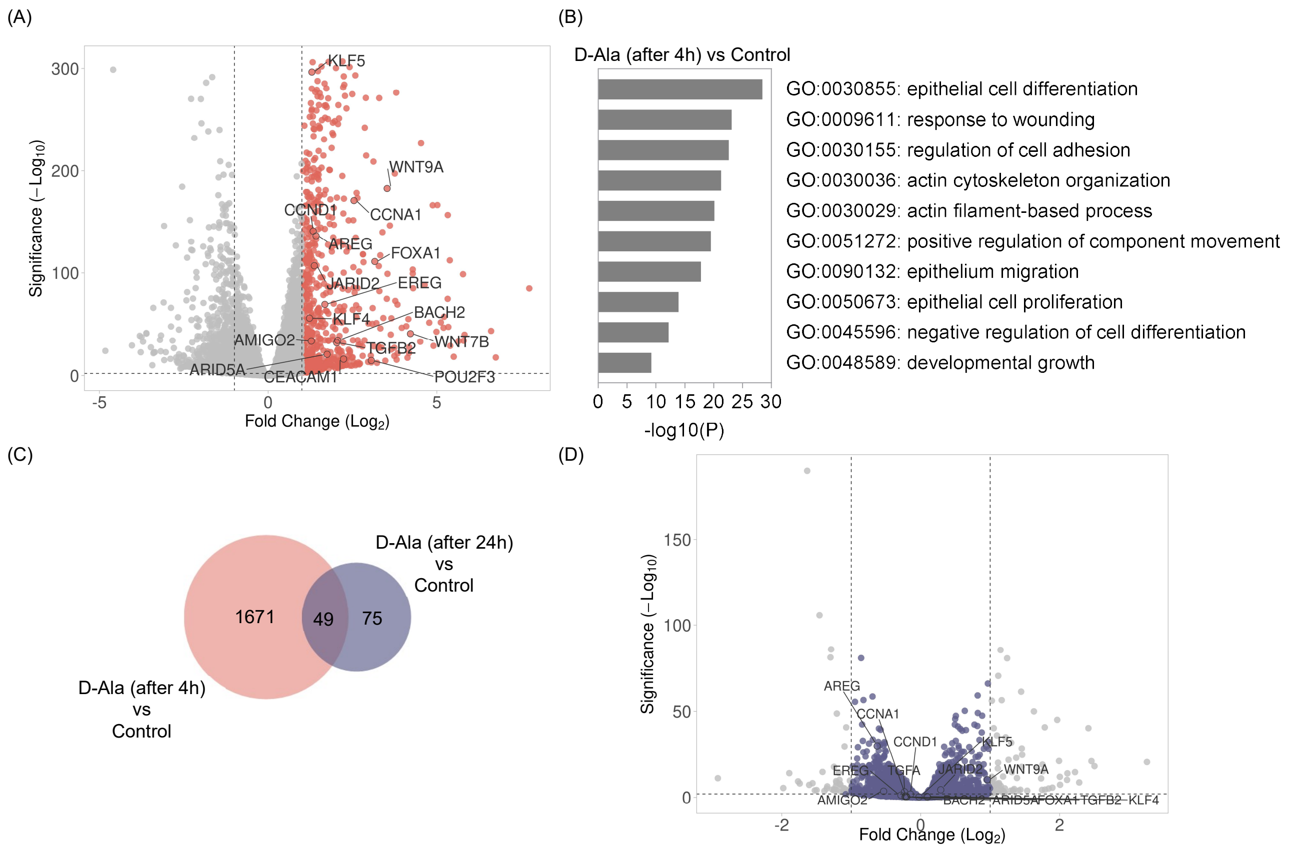

Figure S2. Nuclear H_2O_2 promotes the transcription of plasticity-related genes. *Related to Figure 1.*

(A) Volcano plot of differentially expressed mRNAs identified in MCF10A$^{ER/vSrc}$ cells 4h after treatment with 10 nM D-Ala. Dotted lines in X-axis represent Log_2 (FC) = 1 cut-off.

(B) GO-term enrichment analysis of genes significantly upregulated in MCF10A$^{ER/vSrc}$ cells 4h after treatment with 10 nM D-Ala.

(C) Venn diagram of differentially expressed genes in (4h after treatment with 10 nM D-Ala x Control) vs (24h after treatment with 10 nM D-Ala x Control).

(D) Volcano plot of differentially expressed mRNAs identified in MCF10A$^{ER/vSrc}$ cells 24h after treatment with 10 nM D-Ala. Dotted lines in X-axis represent Log_2 (FC) = 1 cut-off.

(A)

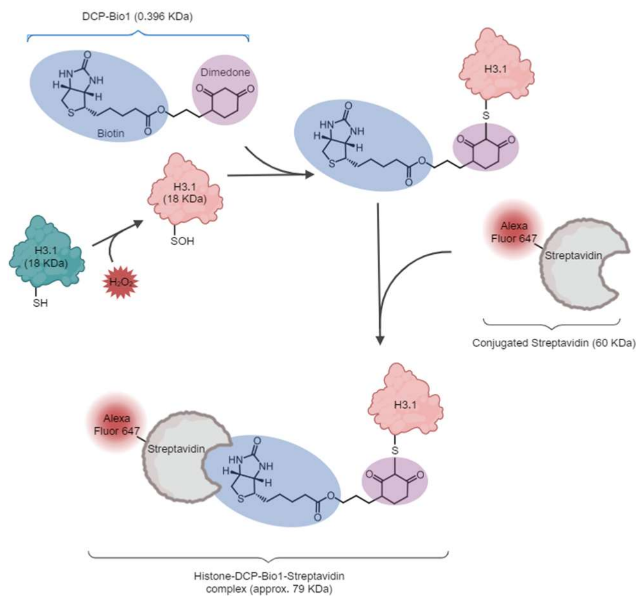

(B)

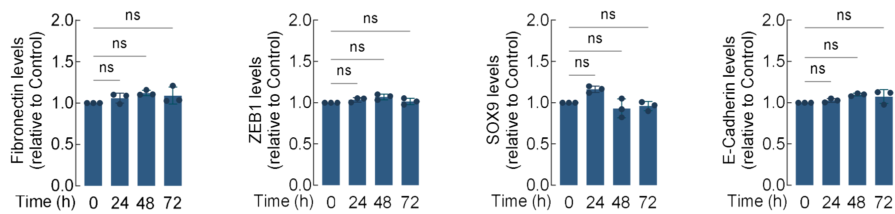

(C)

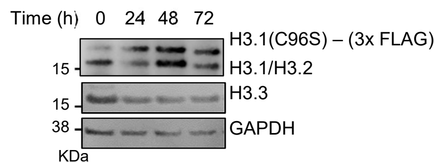

(D)

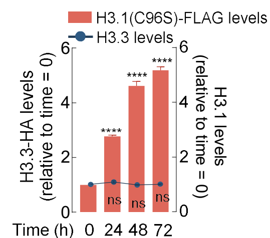

(E)

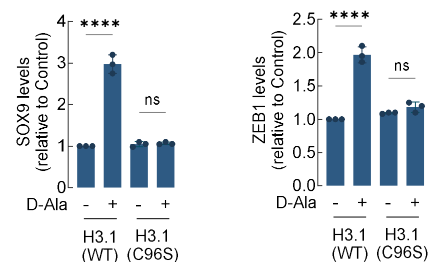

Figure S3. Determining H3.1 sensitivity to oxidation by H_2O_2 *Related to Figure 3.*

(A) Schematic representation cysteine sulfenic acid by DCP-Bio1. Biotin-conjugated DCP-Bio1 is incubated with oxidized recombinant histone variants and forms adducts that can be detected by Alexa-Fluor-conjugated streptavidin.

(B) Quantification of fibronectin, ZEB1, SOX9 and E-Cadherin protein levels in (Figure 3E). Statistical significance was determined by One-way ANOVA multiple comparison test with *post hoc* Tukey test. Bars represent mean ± SEM. ns - not significant.

(C) H3.1(C96S), by itself, does not affect the expression of H3.3. Tetracycline induction of a

TetON inducible-promoter controlling the expression of H3.1(C96S)-FLAG increased H3.1(C96S)-FLAG protein levels without, however, interfering with endogenous H3.3.

(D) H3.3 levels in response to H3.1(C96S)-FLAG overexpression in (C). Statistical significance was determined by One-way ANOVA multiple comparison test with *post hoc* Tukey test. Bars represent mean ± SEM. ****$p<0.0001$, ns - not significant.

(E) Quantification of SOX9 and ZEB1 protein levels in (Figure 3H). Statistical significance was determined by One-way ANOVA multiple comparison test with *post hoc* Tukey test. Bars represent mean ± SEM. ****$p<0.0001$, ns - not significant.

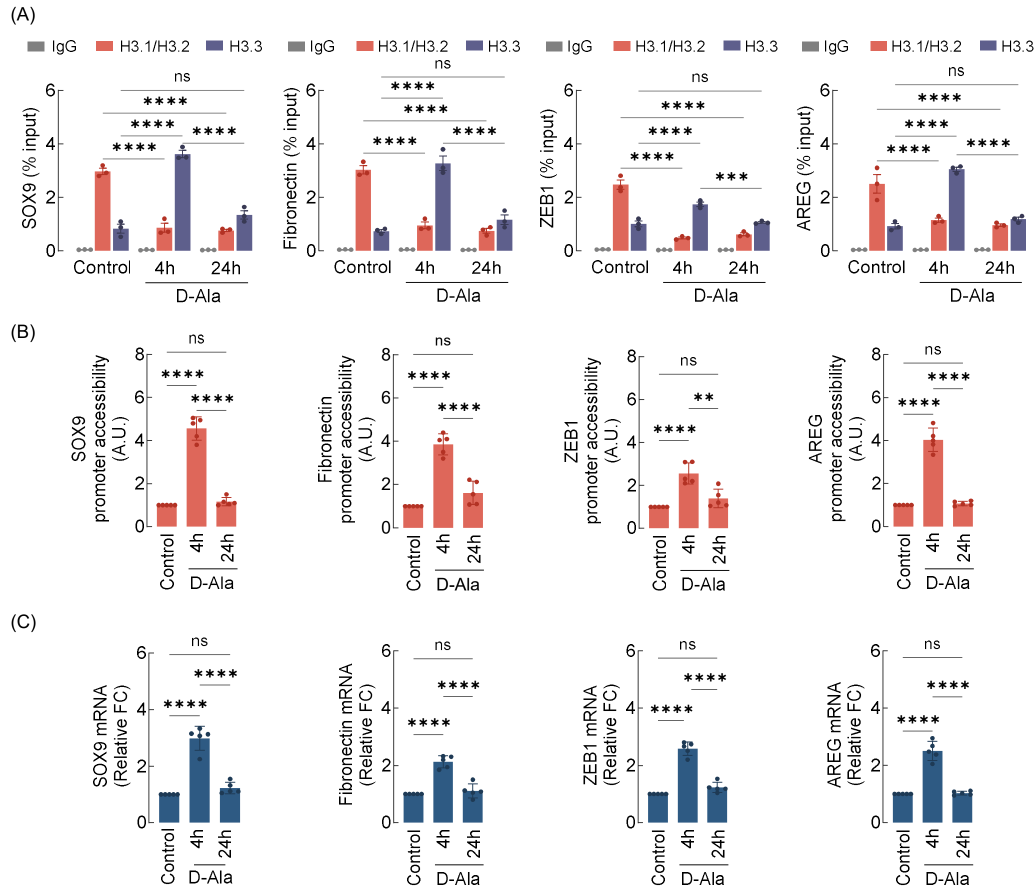

Figure S4. Analysis of histone variants association to promoter regions and consequent changes in promoter accessibility and mRNA transcript levels of genes. *Related to Figure 3.*

(A) H3.1/H3.2 and H3.3 enrichment (ChIP-qPCR) in promoter regions of SOX9, fibronectin, ZEB1 and AREG in MCF10A$^{ER/vSrc}$ cells 4h or 24h after treatment with 10 nM D-Ala. Statistical significance was determined by Two-way ANOVA multiple comparison test with *post hoc* Bonferroni test. Bars represent mean ± SEM. ***p<0.001, ****p<0.0001, ns - not significant.

(B) SOX9, fibronectin, ZEB1 and AREG promoter accessibility in MCF10A$^{ER/vSrc}$ cells 4h or 24h after treatment with 10 nM D-Ala. Statistical significance was determined by One-way ANOVA multiple comparison test with *post hoc* Tukey test. Bars represent mean ± SEM. **p<0.01, ****p<0.0001, ns - not significant.

(C) RT-qPCR analysis of SOX9, fibronectin, ZEB1 and AREG in MCF10A$^{ER/vSrc}$ cells 4h or 24h after treatment with 10 nM D-Ala. Statistical significance was determined by One-way ANOVA multiple comparison test with *post hoc* Tukey test. Bars represent mean ± SEM. ****p<0.0001, ns - not significant.

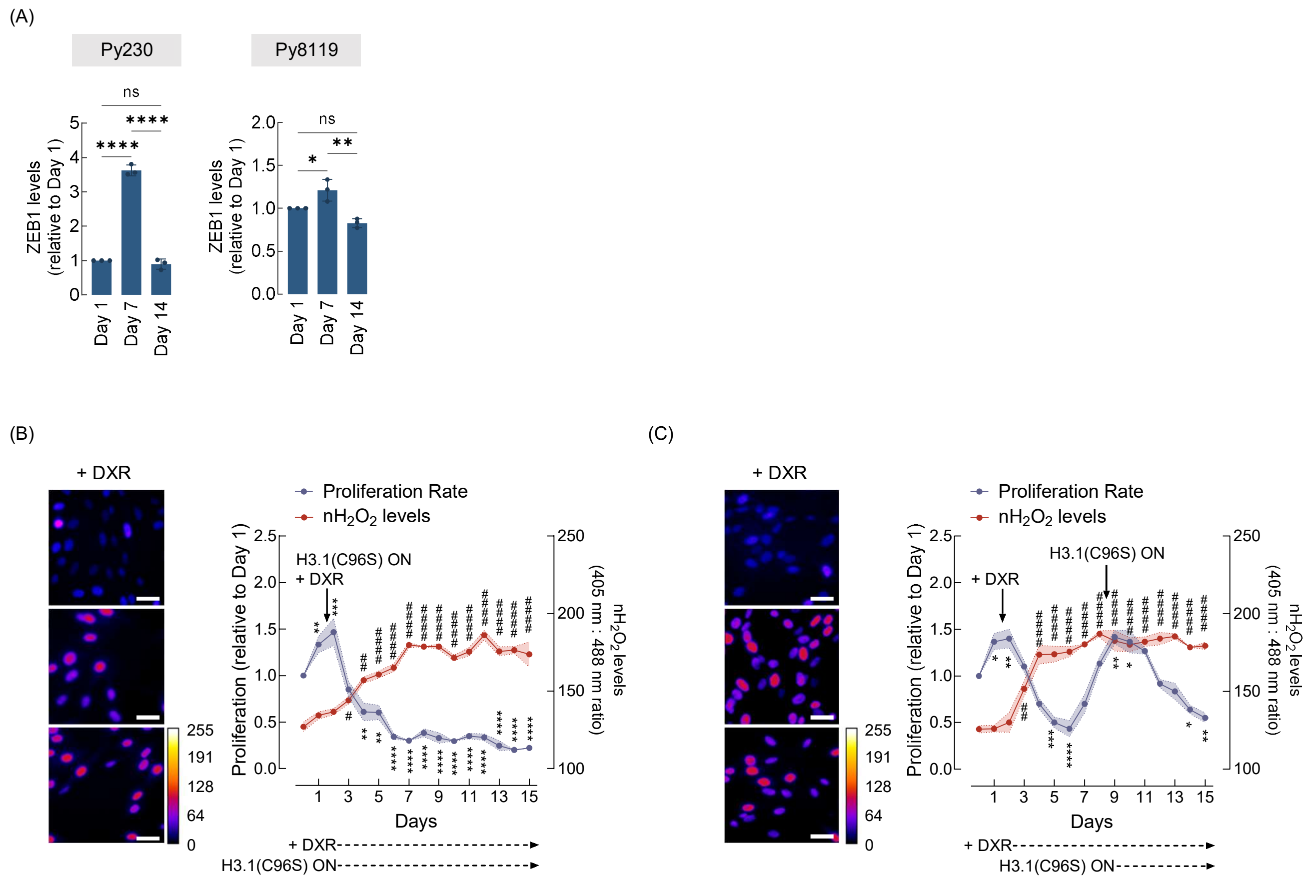

Figure S5. Mutant H3.1(C96S) expression prevents adaptative response to doxorubicin. *Related to Figure 5.*

(A) Quantification of ZEB1 protein levels in (Figure 5G). Statistical significance was determined by One-way ANOVA multiple comparison test with *post hoc* Tukey test. Bars represent mean ± SEM. *p<0.05, **p<0.01, ***p<0.001, ns - not significant.

(B) Induction of H3.1(C96S) expression prior to drug (DXR) treatment prevents chemoresistance development. Cell proliferation and levels of H_2O_2 in the nucleus of MCF10A$^{ER/vSrc}$ cells expressing inducible H3.1(C96S) and treated with 200 nM Doxorubicin (DXR). Oxidized (λ_{ex} = 405 nm) and reduced (λ_{ex} = 488 nm) roGFP2 signals were acquired and the ratio oxidized:reduced was calculated using ImageJ (shown as a heatmap). Cell proliferation was calculated relative to day 1. White bars represent 50 µm. Statistical significance was determined by One-way ANOVA multiple comparison test with *post hoc* Tukey test (with proliferation and nH_2O_2 calculated separately). Lines and shadows represent mean ± SEM. **p<0.01, ***p<0.001, ****p<0.0001 (for proliferation) and $^{\#}$p<0.05, $^{\#\#}$p<0.01, $^{\#\#\#\#}$p<0.0001 (for nH_2O_2 levels).

(C) Induction of H3.1(C96S) expression after DXR-induced chemoresistance resensitizes persister cells to the killing effects of the drug. Cell proliferation and levels of H_2O_2 in the nucleus of MCF10A$^{ER/vSrc}$ cells late expressing inducible H3.1(C96S) and treated with 200 nM Doxorubicin (DXR). Oxidized (λ_{ex} = 405 nm) and reduced (λ_{ex} = 488 nm) roGFP2 signals were acquired and the ratio oxidized:reduced was calculated using ImageJ (shown as a heatmap). Cell proliferation is relative to day 1. White bars represent 50 µm. Statistical significance was determined by One-way ANOVA multiple comparison test with *post hoc* Tukey test (with

proliferation and nH_2O_2 calculated separately). Lines and shadows represent mean ± SEM. $^{*}p<0.05$, $^{**}p<0.01$, $^{***}p<0.001$, $^{****}p<0.0001$ (for proliferation) and $^{\#\#}p<0.01$, $^{\#\#\#\#}p<0.0001$ (for nH_2O_2 levels).

Table S1. List of oligonucleotides used in this study.

RT-qPCR primers	Sequence	Source
ALDH1A3 forward	5'-caccgactatggactcacag -3'	This paper
ALDH1A3 reverse	5'-gggcgttgtagcagttgat-3'	This paper
AREG forward	5'-ccaatgagagccccgctg-3'	This paper
AREG reverse	5'-gagtaggtgtcattgaggtcca-3'	This paper
Fibronectin forward	5'-gggtgacacttatgagcgtcct-3'	This paper
Fibronectin reverse	5'-ggcagcggtttgcgatg-3'	This paper
GAPDH forward	5'-gaagactgtggatggccc-3'	This paper
GAPDH reverse	5'-acctgcccacagcctt-3'	This paper
KLF4 forward	5'-ccacatgaagcgacttcccc-3'	This paper
KLF4 reverse	5'-ttgctaccgccgcaagc-3'	This paper
SOX9 forward	5'-tccagcgaacgcac-3'	This paper
SOX9 reverse	5'-gttgaaggggctgtaggc-3'	This paper
TGFA forward	5'-ggctggacagctcgcc-3'	This paper
TGFA reverse	5'-ctgctgcagccacggg-3'	This paper
WNT7A forward	5'-gctcacaaatgggcctggac -3'	This paper
WNT7A reverse	5'-ctttgagctccttcccgaagac-3'	This paper
ZEB1 forward	5'-ggcaatttgtctcctagtcagc-3'	This paper
ZEB1 reverse	5'-ttgagagctcttctgcacttgg-3'	This paper
ChIP-qPCR and chromatin accessibility assay qPCR primers		
AREG forward	5'-gctaacatcactaagcca-3'	This paper
AREG reverse	5'-cagccctgattacg-3'	This paper
Fibronectin forward	5'-tccacccgaagagaggtg-3'	This paper
Fibronectin reverse	5'-cacgggggactgtgg-3'	This paper
SOX9 forward	5'-ccctcctcctcctctccaa-3'	This paper
SOX9 reverse	5'-taccgcggcgagcactta-3'	This paper
ZEB1 forward	5'-gccgagcctccaacttt-3'	This paper
ZEB1 reverse	5'-tagggaccgggcggttt-3'	This paper